Hindawi
Shock and Vibration
Volume 2023, Article ID 4904326, 10 pages
https://doi.org/10.1155/2023/4904326

Research Article

Study on Sound Propagation Performance of Mechanized Coal Gangue-Fine Sand Filling Body

Daiqiang Deng,[1] **Jinkuan Fan**,[1] **Guodong Cao**,[1] **Yihua Liang**,[2] **Runze Wang**,[1] **Yu Gao**,[1] **and Yunfan Ma**[1]

[1]*College of Civil Engineering, Xiangtan University, Xiangtan 411105, China*
[2]*Industrial Development Research Center of Guizhou, Guizhou Institute of Technology, Guiyang, Guizhou 550003, China*

Correspondence should be addressed to Guodong Cao; gdcao@xtu.edu.cn and Yihua Liang; 20150631@git.edu.cn

Received 9 March 2023; Revised 9 May 2023; Accepted 18 May 2023; Published 5 June 2023

Academic Editor: Pengfei Wang

In the process of continuous and high-intensity mining in soft rock coal mines, high-quality filling treatment is required for the goaf. A nondestructive acoustic velocimetry method is an excellent way to measure the quality of filling body to effectively maintain the rock stability of the mining area and decrease industrial solid waste. In this study, the gangue and fine sand are used as the filling aggregates, and the uniaxial compression test and acoustic wave test are conducted in the cementitious gangue-sand filling body with different gangue-sand ratio. The results show that the longitudinal wave velocity of the filling body is basically between 1.556 km/s and 2.413 km/s. When the gangue-sand ratio is small, and the slurry concentration is high, the early strength of the cementitious gangue-sand filling body is low, but the later strength has a good growth trend. For specimens with higher strength-filled bodies, the propagation speed of sound waves inside them is also faster, indicating a certain positive correlation between the strength of the filled body and the speed of sound waves. A mathematical equation using longitudinal wave velocity to predict the strength of filling body is established. This equation can be used to predict and judge the quality of the filling body in the mining area.

1. Introduction

For some coal veins overlaid unique stratigraphic structures, the mining conditions are technically tricky due to the complexity and variability of the strata. For example, in the sharply inclined coal seams mining stage, the overburden displacement characteristics encountered are hypothesized and calculated by combining the long-walled comprehensive mining workings in medium-thick coal seams, and the overburden transport law obtained is in good agreement with the field conditions [1–3]. In the coal seam damage process in coal mining working face under significant mining height conditions, the researchers analyzed the force characteristics of large coal walls based on field observation and theoretical research. They proposed feasible control measures for reducing coal wall destabilization damage [4, 5]. In the various stages of coal mining in the plains and mountains of different scales, many empty areas are produced because coal is continuously mined out, and the mechanical function of the surrounding rock body will gradually deteriorate with time. The stress on the rock layer will be redistributed with coal mining. During development of a particular stage, the rock body will be sharply displaced towards the mining area, and then the surrounding rock will collapse and cause the surface collapse, which often disturbs the average production of coal enterprises and brings a series of safety and social problems, so some researchers have carried out analysis for the surface collapse problem, using synthetic aperture radar to observe the surface collapse, summarize the law and take specific measures, and analyze the data, which provide an accurate early warning and judgment decision. [6, 7].

For the ground subsidence caused by coal mining, the Quang Ninh coal mine in Vietnam used Sentinel-1 radar observation technology to monitor and predict the gradual development of subsidence in real-time, and the data

obtained can be used to guide subsequent disaster prevention and mitigation decisions [8]. In order to cope with the great danger brought by the collapse of the roof rock in the mining area, relevant researchers have conducted a lot of field tests and theoretical analysis. The use of solid waste to fill the goaf has an excellent effect on the prevention and control of surface collapse in the maintenance of roof strata. For the study of the mechanical characteristics of the use of gangue-filled quarry areas, the researchers analyzed the force situation of loose gangue under waterlogging conditions while investigated the effect of different factors on the deformation and crushing characteristics of loose gangue filling materials. The conclusions provide a theoretical basis for applying loose gangue filling [9]. In recent years, related research has involved the cementation law of colloidal gangue-fly ash filler, and the complex interaction between pressure and thermodynamics is considered comprehensively in mechanical testing. The THMC coupling model with high applicability is successfully established [10]. In filling mining to control rock dynamics disaster and sand-based cemented filler performance optimization, the researchers summarized the laws of surrounding rock movement in underground and open-pit mining in combination with site conditions. They improved the performance index of the filler by optimizing the combination of filling materials [11–14].

In the area of compaction and homogeneity testing of porous materials such as engineering rock and concrete, researchers have explored the correlation between acoustic properties and strength, density, and other indicators using the acoustic propagation properties of materials, and the findings can be used to guide material performance analysis [15, 16]. Regarding concrete and rock quality inspection techniques, researchers combine the sound propagation properties of materials to compare the similarities and differences between intact and defective materials, thus making reasonable judgments about material integrity [17, 18]. Among the methods for integrity testing of various types of cemented and uncemented fillings, researchers have used the mechanical characteristics of poor concrete-like materials to obtain the sound propagation pattern of fillings with the help of conventional concrete material testing methods [19–22]. Gangue, as a filling aggregate, has its characteristics. Through analyzing the gangue filling body pressure process of acoustic emission performance, researchers explore the technical ways to mitigate the filling body from damage [23, 24]. Soft rock mine has low strength of surrounding rocks and poor overall integrity of local rock masses. In the continuous mining of soft rock coal mines, high-quality filling treatment is required for the extraction area. Applying the acoustic velocity measurement method to the nondestructive testing of the quality of the filling body is an excellent way to effectively maintain the stability of the rock formation.

In this paper, the acoustic characteristic analysis of mechanism gangue-sand filling body is performed to seek relationship between the strength of filling body and parameters of acoustic velocity to provide a viable technical basis for filling material performance. The bulk coal gangue as filling aggregate is applied to the filling management of the mining area, which can make the most important solid waste of coal mining enterprises resource utilization, thus creating good economic benefits and ecological and environmental benefits for the enterprise, while minimizing the harm caused by the solid waste containing harmful elements.

2. Materials and Test Methods

2.1. Mechanism Coal Gangue. The mechanism gangue used in the test was taken from a coal mine in Pu'an County, Liupanshui City, Guizhou Province. Using a small jaw crusher to mechanically crush large pieces of coal gangue, according to the characteristics of the filling process technology, the maximum aperture of the discharge screen of the jaw crusher is 10 mm. The black block gangue is crushed into 0~10 mm. Through the relevant geotechnical performance tests and principles of calculation, the performance of the crushed fine-grained gangue is shown in Table 1.

2.2. Fine Sand. In order to facilitate the collection of test materials, the fine sand is conventional yellow sand for construction. Its main component is siliceous quartz sand, whose properties are shown in Table 2.

2.3. Cement. The PO 42.5-grade ordinary silicate cement is used as the filling cementitious material. The physical performance index is measured; the results are shown in Table 3.

2.4. Water. The mixed water of the filling slurry is tap water coming from Xiangtan City Water Works. The pH value of water is 7.13.

3. Preparation of Filling Slurry

The slump test of filling slurry with different mix proportion was conducted. Based on the slurry flow characteristics, the appropriate aggregate ash ratio (AA) (gangue and fine sand to cement mass ratio), filling slurry concentration (SC), and gangue sand mass ratio (GS) were determined. 3 group tests of different mix proportions were performed. Every group has 3 filling slurry concentration, as shown in Table 4.

According to the requirements of coal mine filling technology, while ensuring pump pressure delivery, it is necessary to minimize the water consumption of the filling slurry to reduce the negative impact of water on the underground mining rock mass. In terms of the mechanical and flow properties of the filling material, considering the connection between mining and filling during coal mining, it is necessary to accelerate the progress of the mining and filling cycle. Therefore, while fully utilizing self-produced solid waste, it is necessary to improve the early strength of the filling material and adopt a material formula that is conducive to improving the fluidity of the filling material slurry and the early strength of the filling material. The slurry concentration (SC) of the three groups are, respectively, 86%, 84%, and 82%, and the aggregate ash ratio (AA) is 3.5 : 1. The gangue sand ratio (GS) is 3 : 7, 5 : 5, and 7 : 3. According to the mix proportion in Table 5, the filling slurry was prepared

Table 1: Physical properties of mechanism gangue.

Specific gravity	Loose bulk density ($kN \cdot m^{-3}$)	Dense bulk density ($kN \cdot m^{-3}$)	Maximum porosity (%)	Minimum porosity (%)	Angle of repose (°)
2.65	15.848	17.456	41.31	32.78	29.36

Table 2: Physical properties of fine sand.

Specific gravity	Loose bulk density ($kN \cdot m^{-3}$)	Dense bulk density ($kN \cdot m^{-3}$)	Maximum porosity (%)	Minimum porosity (%)	Angle of repose (°)
2.51	14.776	16.308	39.68	33.43	30.40

Table 3: Physical properties of P·O 42.5 grade cement.

Specific gravity	Loose bulk density ($kN \cdot m^{-3}$)	Dense bulk density ($kN \cdot m^{-3}$)	Maximum porosity (%)	Minimum porosity (%)	Angle of repose (°)
3.11	9.528	17.271	68.63	43.15	30.40

Table 4: Mix proportion of filling slurry.

Group	Test sample	SC (%)	AA	GS	Material consumption per unit volume ($kg \cdot m^{-3}$)			
					Coal gangue	Fine sand	Cement	Water
	1	86			433.2	1010.9	412.6	302.2
One	2	84		3 : 7	412.0	961.5	392.4	336.3
	3	82			392.0	914.6	373.3	368.7
	4	86			727.1	727.1	415.5	304.4
Two	5	84	3.5 : 1	5 : 5	691.2	691.2	395.0	338.5
	6	82			657.4	657.4	375.6	371.0
	7	86			1025.0	439.3	418.4	306.5
Three	8	84		7 : 3	974.3	417.5	397.6	340.8
	9	82			926.2	396.9	378.0	373.4

Table 5: Main parameters and indicators adopted in the test.

Item	Sampling length (K)	Trigger way	Attenuation multiplier	Sampling frequency	Transmit power (μs)	Low cutoff frequency	High cutoff frequency
Value	1	Microcomputer trigger	1.00	1 MHz	5	100 Hz	1 MHz

in the laboratory and then square specimens of $70.7 \times 70.7 \times 70.7$ mm was formed. After the specimens reach the final set state, they are remolded and placed in the laboratory maintenance box for regular moisture maintenance.

4. Testing and Analysis of Sound Propagation Performance

4.1. Sonic Test Instrument. Ultrasonic technology has obvious unique advantages in nondestructive test. In this paper, the used instrument is a multifunctional acoustic wave tester, as shown in Figure 1. The main components of the instrument include the host, transducer, transmission line, and power supply. The advantages of the instrument are as follows [25, 26].

(1) Developed and researched based on WINDOWS system, parameter setting, and data acquisition controlled by computer

(2) Combined with the LABVIEW virtual instrument development platform, it can meet various needs of users in different situations

(3) The instrument hardware is highly integrated, all components contained in a unique toolbox, which is easy to carry and store

(4) The instrument's software also has various functions, such as waveform display and spectrum analysis, providing excellent convenience for subsequent data processing

In order to accurately measure the longitudinal wave velocity of the filling body, in this acoustic wave test, the multifunctional acoustic wave tester was routinely calibrated. Specific main parameters were also set according to the applicable conditions and material properties, as shown in Table 5.

4.2. Acoustic Test Principle and Test Device. The working principle of the multifunction acoustic wave tester is that a high-voltage pulse generator generates a voltage signal, then digitized by an A/D converter, making it evident through an amplifier, and finally transmitted to the sampling

Figure 1: Multifunctional acoustic wave tester.

Figure 2: Filled body acoustic field test.

by the transmitter [27, 28]. The receiver receives the analog signal in transmission. It is digitized in an A/D converter, followed by a data collector that amplifies it and automatically collects and stores it in the instrument.

Following the acoustic wave test procedure, the preparation of the acoustic propagation velocity test of the cemented filling body was carried out. When using butter as a coupling agent, it is necessary to prepolish the filling specimens with rough ends to avoid the negative effects caused by uneven contact surfaces. During the test, the butter was added between the transducer and the specimen to eliminate the air bubbles, so that there is good contact between the transducer and the specimen. The test result is thus more accurate [29, 30]. The filling body acoustic field test is shown in Figure 2.

4.3. Variation Law of Longitudinal Wave Velocity. The original data of the acoustic wave test of the filling body obtained in this test are processed on the Origin software to restore the test waveform. The No. 3 specimen with a curing age of 5 d is taken as an example, as shown in Figure 3. Use the origin software function to check the travel time Δt of the longitudinal wave in the filling body, and then use equation (1) to calculate the longitudinal wave velocity V_p:

$$V_p = \frac{L}{\Delta t}. \tag{1}$$

The results of the acoustic wave velocity test are shown in Table 6. It can be seen that the maximum longitudinal wave velocity of the filled body test is 2.413 km/s and the minimum is 1.556 km/s. According to further analysis, the wave velocity change of the filling body during the solidification and hardening process (5 d~10 d curing age) was obtained, as shown in Figure 4. It can be seen that the wave velocity has increased with the curing age for three groups. With advance of hydration of cement, the water and air in the specimen are continuously reduced. The original pores are gradually filled and compacted by the hydration products and the compactness increases. Thus, the longitudinal wave velocity of the specimen shows an increasing trend.

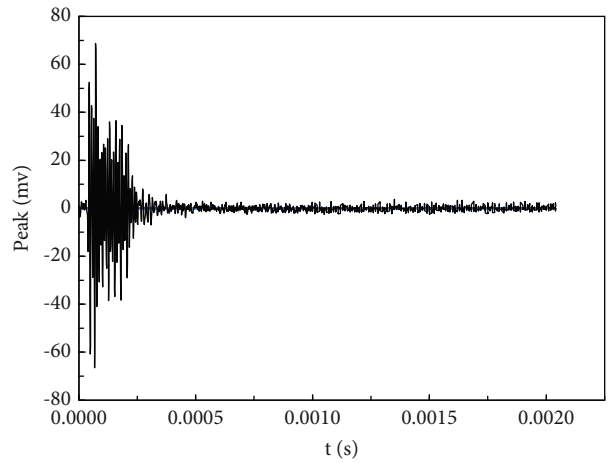

Figure 3: Specimen 5 d sonic test waveform (No. 3).

4.4. Analysis of Sound Propagation Performance in Filling Body

4.4.1. Relationship between Longitudinal Wave Velocity and Strength. According to the acoustic test of the mechanism gangue-fine sand filled specimen, there is a certain regularity between the longitudinal wave velocity and uniaxial compressive strength, as shown in Figure 5. It can be seen that the uniaxial compressive strength has a positive correlation with acoustic wave velocity. After using exponential, linear, logarithmic, and polynomial functions to analyze the data, it was finally found that a good fitting result could be obtained by using the four-term function, and the correlation coefficient R^2 reached above 0.98. This shows that it is accurate and reasonable to predict the uniaxial compressive strength by using the longitudinal wave velocity of the acoustic wave. The equation is shown in equation (2), and the parameters B_1, B_2, B_3, and B_4 in the corresponding analytical expressions have the corresponding optimal values, as shown in Table 7.

$$S_{up} = B_1 V_{up} + B_2 V_{up}^2 + B_3 V_{up}^3 + B_4 V_{up}^4, \tag{2}$$

where S_{up} is the uniaxial compressive strength of the backfill specimen and V_{up} is the longitudinal wave velocity. The B_1, B_2, B_3, and B_4, are coefficients related to the filling body.

Table 6: Sound wave velocity of filling body specimens in each curing age.

Curing age (d)	V_p/ (km/s)								
	1	2	3	4	5	6	7	8	9
5	1.795	1.892	1.750	1.944	1.795	1.667	1.892	1.707	1.556
6	1.892	1.944	1.944	2.059	1.892	1.795	2.059	1.842	1.591
7	2.208	2.000	1.818	2.059	1.842	1.750	1.707	1.707	1.591
8	2.258	2.058	1.842	2.187	2.000	1.556	2.121	1.889	1.647
9	2.413	2.121	2.058	2.333	2.059	1.892	2.147	2.108	1.707
10	2.413	2.187	2.058	2.500	2.187	1.944	2.180	2.108	1.794

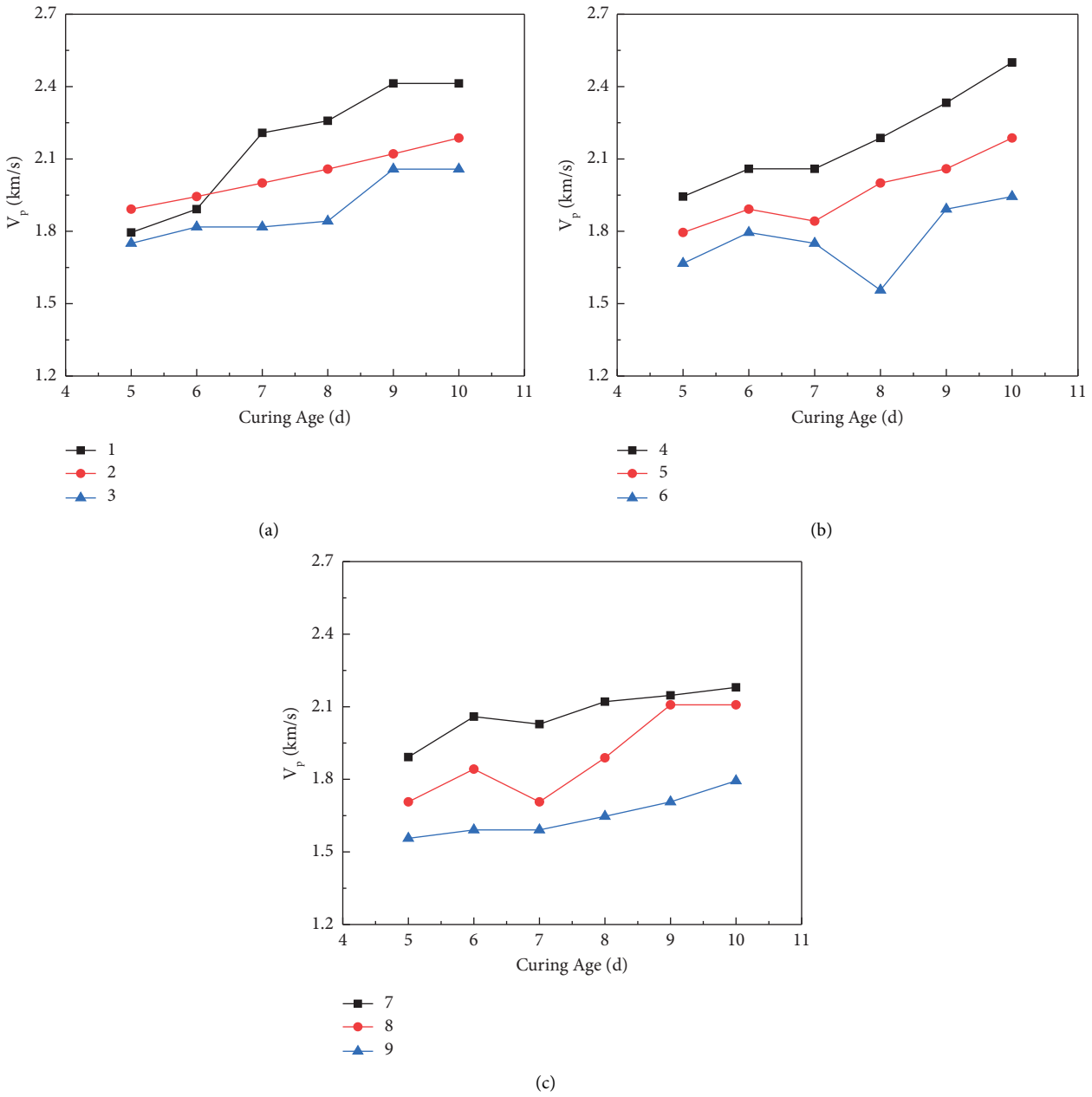

Figure 4: P-wave velocity of each group of backfill specimens: (a) test samples 1~3, (b) test samples 4~6, and (c) test samples 7~9.

4.4.2. Effects of Slurry Concentration on Longitudinal Wave Velocity. The relationship curve between the longitudinal wave velocity and the slurry concentration (SC) is shown in Figure 6. For gangue-sand ratio (GS) of 3 : 7, when the maintenance age is 5 d and 6 d, the slurry concentration (SC) and the strength of the filling body are not significantly

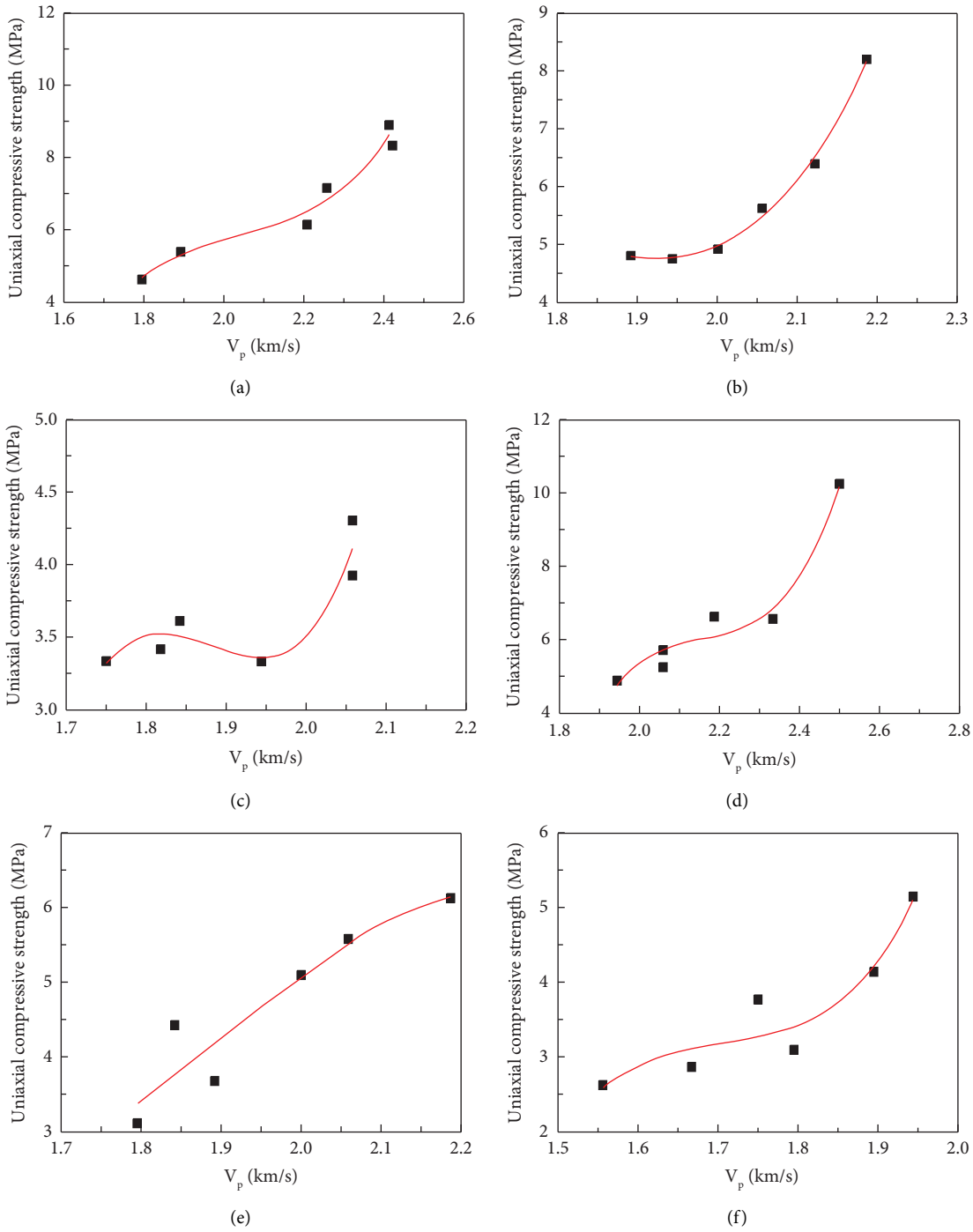

Figure 5: Continued.

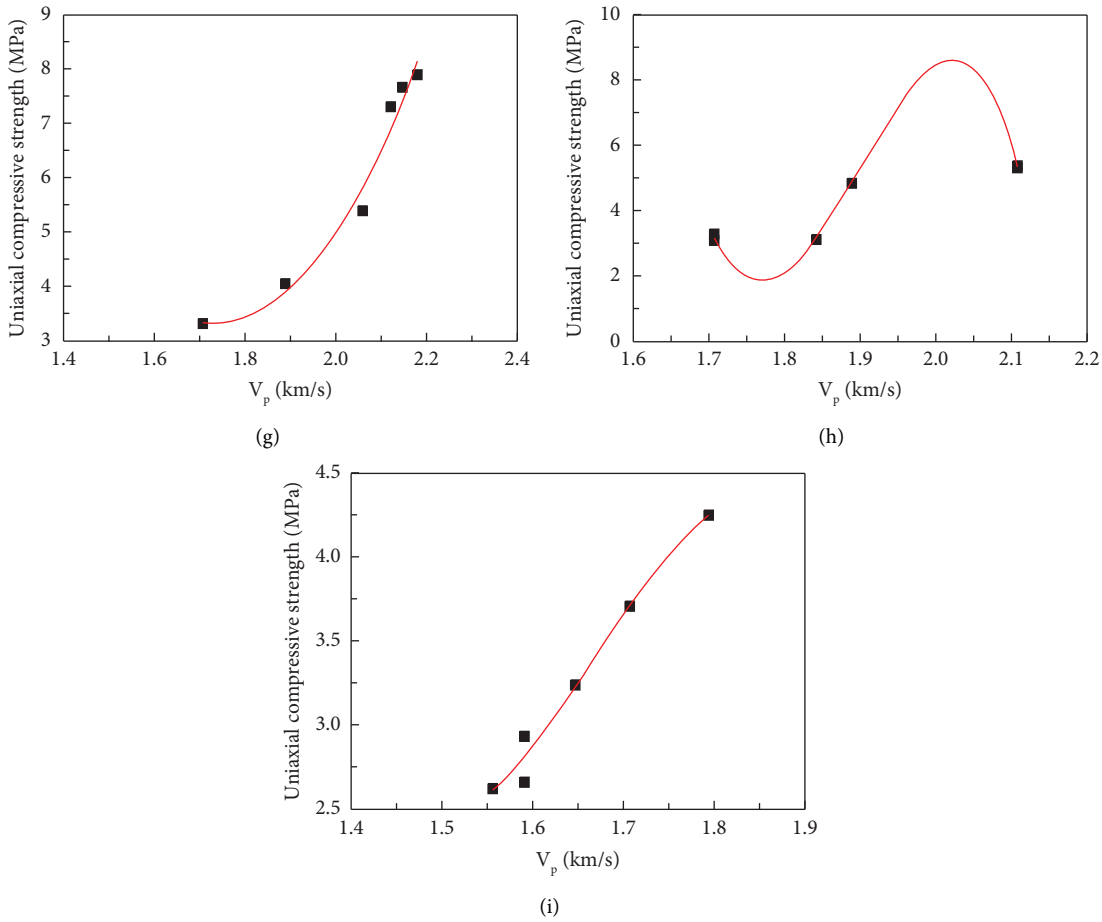

Figure 5: Relationship between strength and wave velocity: (a) test sample 1, (b) test sample 2, (c) test sample 3, (d) test sample 4, (e) test sample 5, (f) test sample 6, (g) test sample 7, (h) test sample 8, and (i) test sample 9.

Table 7: Parameter values and correlation coefficients of each curve fitting function.

Group	Test sample	SC (%)	AA	GS	B_1	B_2	B_3	B_4	R^2
One	1	86		3 : 7	−123.49	184.51	−89.84	14.58	0.99575
	2	84			−93.45	184.84	−113.74	22.65	0.99987
	3	82			−605.62	973.87	−519.34	92.12	0.99651
Two	4	86	3.5 : 1	5 : 5	−364.07	508.50	−234.85	36.14	0.99377
	5	84			55.15	−93.61	52.81	−9.58	0.98319
	6	82			−310.83	548.63	−320.77	62.49	0.98506
Three	7	86		7 : 3	45.89	−53.98	18.89	−1.37	0.99384
	8	84			2992.21	−4774.94	2531.56	−445.54	0.99942
	9	82			277.32	−504.94	306.34	−61.487	0.99825

correlated. The filling body with slurry concentration (SC) of 84% has the highest strength. When the maintenance age exceeds 6 d, the strength of the filling body with the slurry concentration (SC) increases; the strength of the filling body prepared at the 86% slurry concentration (SC) is the highest. It indicates that the early strength of the filling body is low at a low gangue ratio (GS) and high slurry concentration (SC), but later it has good growth. When there is sufficient time on site, a lower gangue ratio (GS) can be used to prepare the mechanism coal gangue-fine sand backfill material to fill and treat goaf in mine.

In addition, for 5 : 5 or 7 : 3 gangue-sand ratio (GS), it can be seen that almost all acoustic longitudinal wave velocity increases with the slurry concentration (SC) in each curing age, which indicates that in the condition of larger gangue-sand ratio (GS), for the same hydration reaction time, the strength of filling body increases with the slurry concentration (SC). In the subsequent experimental test, the optimal filling material formulation can be sought in the higher gangue-sand ratio (GS) filling material.

In this test, no measures and means were taken to reduce and eliminate the relevant effects, so individual discrepancy

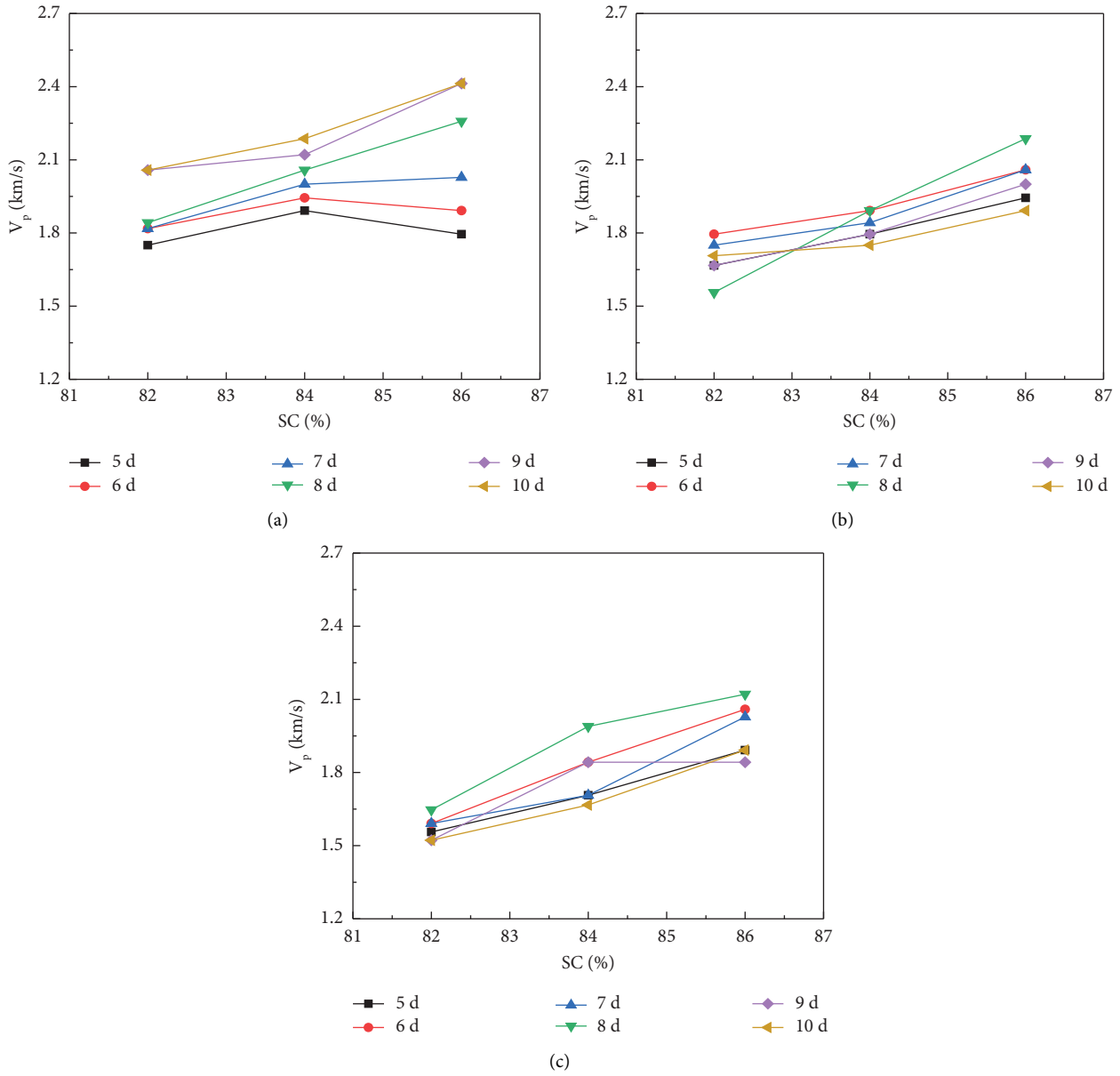

Figure 6: The relationship between the slurry concentration (SC) and the wave speed of the backfill specimen: (a) (GS) 3 : 7, (b) (GS) 5 : 5, and (c) (GS) 7 : 3.

data appeared in the acoustic test curve of the filled body. In future studies, the number of test groups can be further expanded to avoid the analytical bias caused by discrete data as much as possible.

5. Conclusions

In this study, the filler specimens with different slurry concentration (82, 84, and 86%) and gangue-sand ratio (GS) were made. Through the acoustic wave test, the law of longitudinal wave velocity in the filling body at different curing ages was analyzed, and the quartic function relationship between the backfill body strength and the longitudinal wave velocity is established.

Gangue ratio (GS), slurry concentration (SC), and curing time (t) are all crucial factors that affect the uniaxial compressive strength of mechanism coal gangue-fine sand backfill. The strength of the backfill increases with the increase of slurry concentration (SC) and curing time (t). When the sand-cement ratio (B) remains unchanged, under the same slurry concentration (E) and curing time (t), the uniaxial compressive strength of the specimen shows a negative growth trend with the increase of the gangue ratio (GS).

By comparing the compressive strength of the mechanism gangue-fine sand backfill with its longitudinal wave velocity data, it is found that the higher the uniaxial compressive strength, the faster the longitudinal wave speed of

the filling acoustic detection. The wave speed range is basically between 1.556 km/s and 2.413 km/s in this test. The quartic function fitting with the correlation coefficient R^2 above 0.98 was performed on the strength of the machine-made coal gangue-fine sand backfill and the longitudinal wave velocity data. The backfill strength can be predicted through this functional relationship.

The longitudinal wave velocity of the filling body was the fastest when the slurry concentration (SC) was 84% before 6 d when the gangue-sand ratio (GS) was 3 : 7. However, the longitudinal wave velocity was the fastest when the slurry concentration (SC) was 86% after 6 d. That is to say, when the gangue-sand ratio (GS) is small and the slurry concentration (SC) is large, the early strength of the prepared mechanism gangue-fine sand filling body is low, and its later growth is good. At the same time, it can be seen that the filling body longitudinal wave velocity increases with the increase of slurry concentration (SC).

In studying sound propagation characteristics of concrete-like materials, gangue concrete's mechanical and acoustic emission characteristics under uniaxial compression were analyzed [31]. Due to the special lithology of coal gangue, it has high porosity and more microscopic cracks, which lead to its low mechanical properties. Thus the strength of coal gangue concrete is lower than that of gravel concrete. Usually, the maximum load-bearing strength of gangue concrete is 35~40 MPa, which is much higher than the strength of the mechanism gangue-fine sand filling body, so in the subsequent study, the relationship between higher strength filling body and its acoustic wave can be investigated. At the same time, in the follow-up test, the gangue can be considered compared to other general filling material characteristics in the acoustic testing process to seek the most optimal solution to reduce adverse effects caused by the lithology of the gangue, porosity, and microscopic fractures of the filling body.

Data Availability

The data used to support the findings of this study are available from the corresponding author upon request.

Conflicts of Interest

The authors declare that they have no conflicts of interest.

Authors' Contributions

Daiqiang Deng, Jinkuan Fan, and Guodong Cao wrote the main text of the manuscript. Yihua Liang, Runze Wang, Yu Gao, and Yunfan Ma collected and analyzed the data. All authors reviewed and commented on the manuscript.

Acknowledgments

This work was supported by the Provincial Natural Science Foundation of Hunan (2023JJ50041), the Doctoral Research Project of Xiangtan University (22QDZ28, 22QDZ35), and the High-Level Talent Gathering Project in Hunan Province (2019RS1059).

References

[1] H. Zhang, X. B Zhang, P. S. Xie, and L. Ding, "Overlying strata migration law of longwall fully mechanized mining face with steely inclined medium-thickness coal seam," *Shaanxi Coal*, vol. 40, no. 1, pp. 22–25, 2021.

[2] X. Deng, Z. Yuan, Y. Li, H. Liu, J. Feng, and B. de Wit, "Experimental study on the mechanical properties of microbial mixed backfill," *Construction and Building Materials*, vol. 265, Article ID 120643, 2020.

[3] S. Ouyang, Y. Huang, H. Gao, Y. Guo, L. Wu, and J. Li, "Study on the distribution characteristics and ecological risk of heavy metal elements in coal gangue taken from 25 mining areas of china," *Environmental Science and Pollution Research*, vol. 29, 2022.

[4] D. Z Kong, Y. Liu, and Q. Z Liu, "Study of coal face failure mechanism of a large-cutting-height mining face," *Chinese Journal of Rock Mechanics and Engineering*, vol. 37, no. 1, pp. 3458–3469, 2018.

[5] D. Z. Kong, Z. B. Cheng, and S. S. Zheng, "Study on the failure mechanism and stability control measures in a large-cutting-height coal mining face with a deep-buried seam," *Bulletin of Engineering Geology and the Environment*, vol. 78, no. 8, pp. 6143–6157, 2019.

[6] F. G. Bell, T. R. Stacey, and D. D. Genske, "Mining subsidence and its effect on the environment: some differing examples," *Environmental Geology*, vol. 40, no. 1-2, pp. 135–152, 2000.

[7] R. Burgmann, P. A. Rosen, and E. J. Fielding, "Synthetic aperture radar interferometry to measure Earth's surface topography and its deformation," *Annual Review of Earth and Planetary Sciences*, vol. 28, no. 1, pp. 169–209, 2000.

[8] V. K. Dang, T. D. Nguyen, N. H. Dao, T. L. Duong, X. V. Dinh, and C. Weber, "Land subsidence induced by underground coal mining at Quang Ninh, Vietnam: persistent scatterer interferometric synthetic aperture radar observation using Sentinel-1 data," *International Journal of Remote Sensing*, vol. 42, no. 9, pp. 3563–3582, 2021.

[9] M. Li, A. Li, J. X. Zhang, Y. Huang, and J. Li, "Effects of particle sizes on compressive deformation and particle breakage of gangue used for coal mine goaf backfill," *Powder Technology*, vol. 360, no. C, pp. 493–502, 2020.

[10] J. Li, Y. L. Huang, M. Qiao et al., "Effects of water soaked height on the deformation and crushing characteristics of loose gangue backfill material in solid backfill coal mining," *Processes*, vol. 6, no. 6, p. 64, 2018.

[11] D. Wu, T. Deng, and R. Zhao, "A coupled THMC modeling application of cemented coal gangue-fly ash backfill," *Construction and Building Materials*, vol. 158, pp. 326–336, 2018.

[12] Y. C. Xue, T. Xu, P. L. P. Wasantha, T. H. Yang, and T. Fu, "Dynamic disaster control of backfill mining under thick magmatic rock in one side goaf: a case study," *Journal of Central South University*, vol. 27, no. 10, pp. 3103–3117, 2020.

[13] N. Zhou, J. X. Zhang, S. Ouyang, X. Deng, C. Dong, and E. Du, "Feasibility study and performance optimization of sand-based cemented paste backfill materials," *Journal of Cleaner Production*, vol. 259, Article ID 120798, 2020.

[14] G. B. Dreher and R. B. Finkelman, "Selenium mobilization in a surface coal mine, Powder River Basin, Wyoming, U.S.A," *Environmental Geology and Water Sciences*, vol. 19, no. 3, pp. 155–167, 1992.

[15] Z. F Liu and B. Yan, "Propagation and evolution of acoustic waves in porous materials," *Chinese Journal of Applied Mechanics*, vol. 1, pp. 41–158, 1999.

[16] J. P. Wu, "Study on the compressibility of unconsolidated sandstone based on acoustic logging data," *Journal of Xi'an Shiyou University(Natural Science Edition)*, vol. 24, no. 03, pp. 49–51, 2009.

[17] M. J Zhao and D. L Wu, "Ultrasonic classification and strength prediction of engineering rock mass," *Chinese Journal of Rock Mechanics and Engineering*, vol. 19, no. 1, pp. 89–92, 2000.

[18] X. B Zhang, X. Y. Zhang, and X. Fang, "Testing Method of a New Type of Concrete Defects," *China Concrete and Cement Products*, vol. 11, pp. 77–80, 2017.

[19] M. M Hu, Y. Gao, J. Q. Chen, and D. X. Si, "Study on Real Time Synchronized Correlation between Wave Velocity and Stress of Pea-gravel Backfills," *Modern Tunnelling Technology*, vol. 57, no. 03, pp. 135–140, 2020.

[20] H. Zhao, A. Fuller, W. Thongda et al., "SNP panel development for genetic management of wild and domesticated white bass (Morone chrysops)," *Animal Genetics*, vol. 50, no. 1, pp. 92–96, 2019.

[21] H. L. F. Study, "On the Stability of Cemented Backfill of Block Stone," *China Mine Engineering*, vol. 4, pp. 22–27, 1996.

[22] S. L. Li, J. H. Mao, and Y. F. Sang, "Investigation on the backfill status of Fankou Lead-Zinc Mine," *Hunan Nonferrous Metals*, vol. 2, pp. 22–25, 1996.

[23] D. Wu, R. Zhao, and C. Qu, "Effect of Curing Temperature on Mechanical Performance and Acoustic Emission Properties of Cemented Coal Gangue-Fly Ash Backfill," *Geotechnical and Geological Engineering*, vol. 37, no. 4, pp. 3241–3253, 2019.

[24] G. Q Kong, *Study on Acoustic Emission Characteristics of Crushed Gangues during Confined Compaction*, China University of Mining and Technology, Xuzhou, China, 2019.

[25] G. Yu, *Research on Acoustic Cha Racteristics in the Hardening Process of Concrete*, Xiangtan University, Xiangtan, China, 2019.

[26] S. G. Long and S. F Xiao, "Effect of meshing on concrete ultrasonic CT imaging," *Engineering Journal of Wuhan University*, vol. 50, no. 5, pp. 708–713, 2017.

[27] P. Yan, Y. J. Zou, W. B. Lu et al., "Real-Time Assessment of Blasting Damage Depth Based on the Induced Vibration During Excavation of a High Rock Slope," *Geotechnical Testing Journal*, vol. 39, no. 6, 20150991 pages, Article ID 20150187, 2016.

[28] L. Miranda, L. Cantini, J. Guedes, L. Binda, and A. Costa, "Applications of Sonic Tests to Masonry Elements: Influence of Joints on the Propagation Velocity of Elastic Waves," *Journal of Materials in Civil Engineering*, vol. 25, no. 6, pp. 667–682, 2013.

[29] J. M Zhang, R. Wang, and G. S. Jiang, "Experiment study on grouting soil uniaxial compression strength and its acoustic velocity," *Coal Geology and Exploration*, vol. 5, pp. 33–36, 2003.

[30] Z. Q. Zhu, B. Yu, S. W. Mi, T. Yu, and Y. Zhou, "Ultrasonic attenuation characteristics of ultrasonic in concrete," *Journal of Central South University*, vol. 45, no. 11, pp. 3900–3907, 2014.

[31] M. Xiao, F. Ju, P. Ning, and K. Li, "Mechanical and Acoustic Emission Behavior of Gangue Concrete under Uniaxial Compression," *Materials*, vol. 12, no. 20, p. 3318, 2019.